Published in final edited form as:

Nature. 2016 March 17; 531(7594): 329–334. doi:10.1038/nature16966.

Observing cellulose biosynthesis and membrane translocation *in crystallo*

Jacob L.W. Morgan[a,*], **Joshua T. McNamara**[a,*], **Michael Fischer**[b,c], **Jamie Rich**[b], **Hong-Ming Chen**[b], **Stephen G. Withers**[b], and **Jochen Zimmer**[a,#]

[a]University of Virginia School of Medicine, Center for Membrane Biology, Molecular Physiology and Biological Physics, 480 Ray C. Hunt Dr., Charlottesville, VA 22908, USA

[b]Department of Chemistry, University of British Columbia, 2036 Main Mall, Vancouver, B.C., Canada V6T 1Z1

Abstract

Many biopolymers, including polysaccharides, must be translocated across at least one membrane to reach their site of biological function. Cellulose is a linear glucose polymer synthesized and secreted by a membrane-integrated cellulose synthase. *In crystallo* enzymology with the catalytically-active bacterial cellulose synthase BcsA-B complex reveals structural snapshots of a complete cellulose biosynthesis cycle, from substrate binding to polymer translocation. Substrate and product-bound structures of BcsA provide the basis for substrate recognition and demonstrate the stepwise elongation of cellulose. Furthermore, the structural snapshots show that BcsA translocates cellulose via a ratcheting mechanism involving a “finger helix” that contacts the polymer's terminal glucose. Cooperating with BcsA's gating loop, the finger helix moves ‘up’ and ‘down’ in response to substrate binding and polymer elongation, respectively, thereby pushing the elongated polymer into BcsA’s transmembrane channel. This mechanism is validated experimentally by tethering BcsA's finger helix, which inhibits polymer translocation but not elongation.

Introduction

Cellulose is an abundant structural cell component produced by many organisms, including bacteria, vascular plants and animals[1–4]. It is a linear polymer of glucose molecules joined between their C1 and C4 carbons[5]. Cellulose is synthesized by membrane-integrated

[#]To whom correspondence should be addressed: ; Email: jochen_zimmer@virginia.edu
[*]These authors contributed equally to this work.
[c]Present Address: Sandoz GmbH, Biochemiestrasse 10, A-6250 Kundl, Tyrol Austria

Author contributions: J.T.M. and J.L.W.M. purified and crystallized BcsA-B and performed all crystal soaking experiments. J.T.M. cloned and analyzed all BcsA cysteine mutants. J.T.M. and J.L.W.M. collected and processed diffraction data and built and refined the BcsA-B models. M.F. synthesized the fluorinated and phosphonate UDP-Glc analogues and J.R. and H-M.C. synthesized the UDP-thio-galactose analogues. J.T.M., J.L.W.M. and J.Z. analyzed the data. J.Z. and J.L.W.M. wrote the paper and all authors edited the text.

The authors declare no competing financial interests.

Structure factors and coordinates have been deposited at the Protein Data Bank under entry codes 5EJ1, 5EIY, and 5EJZ.

glycosyltransferases (GTs) that contain 6 to 8 transmembrane helices (TMHs) as well as an intracellular catalytic GT domain[6]. These enzymes polymerize UDP-activated glucose (UDP-Glc)[7,8] into chains thousands of glucose units long[9] and translocate the polymer across the plasma membrane, through a pore formed by their own TM region[10].

Cellulose is also a common biofilm component[2,11] where it is synthesized and secreted via an inner and, in gram-negative bacteria, outer membrane-spanning cellulose synthase complex[3]. At the inner membrane, the catalytic BcsA and membrane-anchored, periplasmic BcsB subunits form a complex sufficient to synthesize and translocate cellulose[7], while transport across the outer membrane likely occurs through the BcsC subunit[12,13].

Processive GTs, including chitin, alginate and cellulose synthases, transfer the glycosyl moiety from a nucleotide-activated sugar (donor) to a specific hydroxyl group of the growing polysaccharide chain (acceptor) by a nucleophilic S_N2-like substitution reaction[14], thereby forming an elongated polymer and nucleoside diphosphate as reaction products. A processive mechanism requires that the elongated polymer is translocated after each glycosyl transfer, such that the polymer's newly added sugar unit becomes the acceptor in a subsequent reaction. Because all known processive GTs are TM channel-forming enzymes[15–17], the translocation of the polymer into the TM channel between catalytic steps also gives rise to secretion.

Previous structural and functional analyses of the *Rhodobacter sphaeroides* BcsA-B complex containing a nascent cellulose polymer revealed the architecture of the active site, its close association with the TM channel, as well as the coordination of cellulose within the channel[10]. In bacteria, cellulose biosynthesis is activated by the signaling molecule cyclic-di-GMP (c-di-GMP)[18], a potent biofilm inducer and allosteric activator of BcsA[19]. Binding of the activator to BcsA's C-terminal PilZ domain allows a "gating loop" to either insert into the catalytic pocket during substrate binding or to retract from it to release the UDP product[20].

Cellulose synthases contain a short helix within the GT domain, termed "finger helix"[20]. The N terminus of the finger helix contacts the polymer's acceptor glucose via an invariant "TED" motif, of which the Asp likely facilitates the deprotonation of the acceptor C4 hydroxyl during catalysis[10,20].

Crystal structures of the catalytically inactive "resting" state of BcsA-B (in the absence of c-di-GMP)[10] and a c-di-GMP-activated structure[20] provided important insights into the architecture and function of processive GTs. Here, we used *in crystallo* enzymology to obtain structural snapshots of a complete cellulose biosynthesis reaction cycle, providing structures of substrate- and product-bound states, and delineating the mechanism by which the elongated glucan is translocated into BcsA's TM channel.

Cellulose synthase elongates the cellulose chain one glucose unit at a time

The previously determined c-di-GMP-activated BcsA-B structure[20] contains a nascent cellulose polymer 18 glucose molecules long whose non-reducing terminal glucose unit rests at the entrance to BcsA's TM channel, which is marked by the invariant Trp383 of the

"QxxRW" motif[20,21]. In this state, BcsA's finger helix is in an ‘up’ position where it points toward the entrance of the TM channel, thereby positioning Asp343, the putative catalytic base, near the C4 hydroxyl of the polymer’s terminal sugar, Fig. 1a. Because BcsA’s active site is empty and the gating loop is retracted from it, this structure represents a state in which the enzyme is poised to initiate a new cycle of chain elongation, hereafter referred to as the “post-translocation state”.

Strikingly BcsA-B is catalytically active *in crystallo*. Incubating BcsA-B crystals with UDP-glucose in the absence of Mg^{2+} (to slow down the reaction) results in the extension of the polymer's electron density by one glucose unit, Fig. 1a. This demonstrates that cellulose elongation occurs via a stepwise addition of glucose units and that Trp383 of the QxxRW motif indeed forms the acceptor-binding site. The elongated polymer points straight into the catalytic pocket, similar to its position in the recently determined resting state of BcsA[10].

BcsA’s finger helix resets in response to polymer extension

Processive cellulose biosynthesis requires that the elongated polymer is translocated after each elongation cycle and the above described *in crystallo* cellulose extension demonstrates that glycosyl transfer and polymer translocation are separate steps.

To identify whether the extended cellulose translocates spontaneously over time, we extended the polymer *in crystallo* as described above, then diluted the substrate 65-fold, and incubated the crystals overnight before harvesting. Under these conditions, the density for the extended polymer continues to protrude into the catalytic pocket, suggesting that this state is stable in the absence of substrate, Fig. 1a. Strikingly, after extending the cellulose polymer, BcsA's finger helix shifts to a ‘down’ position, such that Thr341 and Asp343 of its TED motif again form hydrogen bonds with the polymer’s terminal glucose unit, Fig. 1a.

The finger helix movement is accompanied by the retraction of a small preceding loop with Phe335 at its tip from a hydrophobic pocket underneath the active site, Fig. 1a. The resulting "pre-translocation" state of BcsA-B contains an empty catalytic pocket, a gating loop retracted from the active site, Extended Data Fig. 1, an extended polymer, and a downward pointing finger helix, Fig. 1a.

Cellulose translocation by a coordinated movement of BcsA's gating loop and finger helix

The observed downward movement of BcsA's finger helix in response to cellulose elongation suggests its role in translocation. If crystals containing the above described pre-translocation step are soaked with UDP/Mg^{2+}, UDP binds and the gating loop inserts into the catalytic pocket, Fig. 1b. Additionally, the finger helix returns to the ’up’ position and the density for the polymer's newly-added glucose unit disappears, Fig. 1b, suggesting its translocation into the channel.

To confirm that the elongated polymer is indeed translocated *in crystallo*, we extended the polymer by one unit with the chain-terminating analogue 6-thio-galactose, whose location

can be unambiguously determined based on anomalous X-ray scattering of its sulfur atom. After polymer extension, the 6-thio-galactosyl moiety sits inside BcsA's catalytic pocket; then upon UDP/Mg^{2+} binding and gating loop insertion into the active site, the density of the newly-added sugar disappears, and the thio-galactosyl unit moves into the TM channel next to Trp383, Extended Data Fig. 2, thereby confirming the genuine translocation of cellulose *in crystallo*.

The ability of UDP/Mg^{2+} to induce translocation brings about the question of why translocation doesn't occur immediately after glycosyl transfer when the UDP/Mg^{2+} product is bound at the active site and the gating loop is inserted. All states of BcsA observed thus far either show its gating loop inserted into the active site and the finger helix in the 'up' position, Fig. 1b, or the gating loop retracted from the active site and the finger helix in the 'down' position, if the cellulose polymer is extended[10,20], Fig. 1a. This suggests that the finger helix cannot move to the 'down' position unless the gating loop is retracted from the active site and that in turn gating loop insertion could induce the upward movement of the finger helix. This coupled movement is likely due to steric clashes between the side chain of Ile340, preceding the TED motif of the finger helix, and the gating loop's backbone, Fig 1c. Ile340 is primarily conserved among bacterial cellulose synthases, eukaryotic enzymes usually contain a valine or occasionally a leucine residue at this position, which could perform a similar function. Indeed, BcsA carrying a Val at position 340 shows indistinguishable catalytic activity compared to the wild type enzyme, while an Ile to Leu substitution reduces the apparent activity by about 50%, Fig. 1d. Thr, Ala, Ser, Phe or Trp, however, support only low or background activities, suggesting that gating loop to finger helix coupling requires a fairly rigid, hydrophobic residue at position 340, Fig. 1d.

The movement of the finger helix is required for cellulose translocation

The conformational changes of BcsA described above suggest that its finger helix moves up and down during cellulose translocation. To test this hypothesis, we engineered double Cys BcsA mutants expected to crosslink the finger helix to an amphipathic helix (IF2) above the GT domain[10], Fig. 1a and Extended Data Fig. 3, and screened those mutants for changes in catalytic activity upon oxidation. Introducing Cys residues at positions 338 near the N terminus of the finger helix and 394 at the C-terminal end of IF2 (hereafter referred to as BcsA-2C) results in attenuated catalytic activity compared to the wild type enzyme or single-Cys mutants in inverted membrane vesicles (IMVs). Full activity, however, can be restored upon addition of excess DTT, Fig 2a. Upon purification of BcsA-2C and reconstitution into proteoliposomes, its catalytic activity further decreases to ~20% under non-reducing conditions, Fig. 2b, likely due to complete disulfide bond formation during purification. Addition of the oxidizing reagent tetrathionate does not further decrease the enzyme's apparent activity, yet the catalytic activity robustly recovers with increasing DTT concentrations. The crystal structure of this BcsA-2C mutant reveals that the disulfide bond forms when the finger helix is in the 'up' position, Fig. 2b and Extended Data Fig. 3, similar to its position in the post-translocation state[20].

Additionally, the ability to observe cellulose elongation and translocation *in crystallo* allows us to further delineate how the engineered disulfide bond affects BcsA's activity. Soaking

BcsA-2C crystals with substrate leads to polymer extension as observed for wild type BcsA, demonstrating that glycosyl transfer is not abolished by the mutations, Fig. 2c and d. Subsequently, if those crystals are then incubated overnight under oxidizing conditions, the finger helix remains in the ‘up’ position, revealing that the cross-link prevents the finger helix from resetting to the ‘down’ position, Fig. 2c. Binding of UDP/Mg^{2+} in these crystals, which induces polymer translocation in wild type BcsA within 15 to 45 min, fails to initiate translocation, even after an overnight incubation, Fig. 2d. However, reducing the engineered disulfide bond in the BcsA-2C complex restores the capability of the finger helix to move downwards following polymer extension and, most notably, restores polymer translocation, Fig. 2c and d, thereby directly correlating the movement of the finger helix with BcsA's ability to translocate the polymer.

The product-bound state

Directly after glycosyl transfer, BcsA contains an elongated glucan plus UDP/Mg^{2+} and an inserted gating loop at the active site, as well as the finger helix in the ‘up’ position. This “product-bound” state is accessible through the BcsA-2C mutant described above. Because the engineered disulfide bond tethers the finger helix, UDP/Mg^{2+} can be bound to the active site after polymer extension without inducing translocation.

Alternatively, we observed that incorporating 2-fluoro-substituted glucose into the polymer stabilizes a similar product-bound state. Attempting to trap a “donor-bound” state by using the usually (but not always) unreactive UDP-2-fluoro-glucose as substrate[22,23], we observed that the nascent glucan is elongated. However, the subsequent translocation of this polymer is significantly impeded (but not abolished), which may be due to the loss of a hydrogen bond between Thr341 of the finger helix and the polymer’s terminal C2 substituent, Fig. 1a. Thus, elongating the cellulose polymer with 2-fluoro-glucose in wild type BcsA, then diluting the substrate and soaking in UDP/Mg^{2+} reproduces a similar product-bound state to that obtained for the BcsA-2C mutant. Due to higher quality diffraction data, Extended Data Table 1, we discuss the structure obtained with 2-fluoro-glucose.

The product-bound BcsA structure shows that the catalytic pocket can accommodate both an extended cellulose polymer and UDP/Mg^{2+}, suggesting that the newly added glucose unit can align with the polymer before the gating loop retracts from the active site and UDP is released, Fig. 3. In this position, the only major interactions of the terminal glucose unit are with UDP's β-phosphate as well as Asp246 of the "DxD" motif[6,14] via its C2 or C6 hydroxyl group (depending on its orientation), Fig. 3b.

Of note, the individual glucose units in cellulose are rotated by approximately 180º relative to their neighbors[5,24]. Therefore, during relaxation into the polymer's plane, the newly added glucose moiety must rotate either clock- or counter clockwise to be in register with the preceding glucose units[25,26]. This alternating rotation is most likely driven by the formation of intramolecular hydrogen bonds[26] and could be facilitated by UDP release after glycosyl transfer, which minimizes steric restrictions at the active site, Fig. 3.

The donor glucose binds to a hydrophilic pocket underneath the acceptor

To stabilize the substrate-bound state of BcsA, we synthesized and employed a non-hydrolyzable phosphonate substrate analogue[27], (UDP-CH_2-Glc), in which a methylene bridge connects the donor glucose with UDP's β-phosphate. Additionally, we also capped the cellulose polymer with galactose (see Methods), which cannot be extended due to an axial instead of an equatorial hydroxyl group at its C4 position.

The donor glucose inserts underneath the acceptor into a conserved hydrophilic pocket formed by BcsA's TED, HAKAG and FFCGS motifs, Fig. 4a, and the gating loop cooperates with the QxxRW motif to stabilize the substrate. In particular, the gating loop's Phe503 forms cation-π interactions with Arg382 of the QxxRW motif, which in turn forms a salt bridge with the nucleotide's β-phosphate as well as a hydrogen bond with the donor's C6 hydroxyl, Fig. 4a and b. Further, the donor's C3 hydroxyl interacts with the backbone carbonyl of Cys318 of the FFCGS motif and its ring oxygen is in hydrogen bond distance to the Nε of Trp383 of the QxxRW motif, Fig. 4b. Thus, the recognition of the donor's C3 and C6 hydroxyls and its ring oxygen appears particularly important for substrate selectivity.

In the substrate-bound state, BcsA's finger helix is in the 'up' conformation and positions Asp343 of the TED motif within 2.5 Å of the acceptor's C4 hydroxyl group, consistent with its likely function as general base during catalysis, Fig. 4b. However, the distance between the acceptor and the donor's C1 carbon is about 4.2 Å (assuming glucose instead of galactose as the polymer's terminal sugar), which is likely too far for a direct transfer. We note that the pyrophosphate group of UDP-CH_2-Glc is less deeply inserted into the active site compared to UDP in the product-bound state, Extended Data Fig. 4, perhaps due to the substrate's methylene-bridge and/or the capping of the glucan with galactose. Repositioning UDP-CH_2-Glc according to the UDP conformation in the product-bound state places the donor's C1 carbon within approximately 2.9 Å of the acceptor's C4 hydroxyl, a suitable distance for glycosyl transfer[29], Fig. 4c. This distance is likely also maintained when the acceptor is in the opposite orientation (as is the case for every other glucose unit), due to repositioning of the terminal glucose unit at the active site.

Implications for cellulose biosynthesis and membrane translocation

Cellulose biosynthesis requires that BcsA binds the substrate, positions it for and catalyzes glycosyl transfer, translocates the extended polymer, and exchanges UDP with UDP-Glc for a subsequent elongation cycle. Our structural snapshots of a complete cellulose biosynthesis cycle suggest that BcsA accomplishes this in three steps, Fig. 5.

Upon substrate binding, BcsA's gating loop inserts into the catalytic pocket, thereby positioning the donor glucose for transfer and perhaps also stabilizing the UDP leaving group, Fig. 5. In this state, the acceptor glucose rests next to Trp383 at the entrance to the TM channel and interacts with the TED motif at the N terminus of the finger helix. After glycosyl transfer, the newly added glucose unit aligns with the polymer and extends into the catalytic pocket next to UDP's pyrophosphate group. In this product-bound state, the gating loop remains inserted into the active site and the finger helix continues to point 'up' as

observed in the substrate-bound state. Next, BcsA's gating loop retracts to release UDP and the finger helix resets to the 'down' position to interact again with the polymer's terminal glucose unit. Binding of a new substrate molecule to this pre-translocation state could elicit the translocation of the extended polymer (by an upward movement of the finger helix) through re-insertion of the gating loop into the active site. *In crystallo* translocation experiments with a galactose-capped polymer and UDP-Glc as substrate confirmed that the polymer can indeed be translocated when UDP-Glc/Mg^{2+} binds to the active site (Extended Data Fig. 5). An alternative, perhaps slower, pathway could be the translocation of the polymer prior to substrate binding, facilitated either by random cycles of gating loop insertion and retraction or favorable interactions of the polymer in the extracellular milieu.

How could the opening of the gating loop and resetting of the finger helix be coordinated? The retraction of the gating loop after glycosyl transfer could be facilitated by the rotation of the newly added sugar into the plane of the polymer. Alternatively, it is possible that the Mg^{2+} coordination changes after glycosyl transfer, which in turn could affect the stability of UDP and the gating loop at the active site, as proposed for non-processive galactosyl transferases[30].

BcsA's finger helix is capped at its N terminus by the TED motif, which is invariant among cellulose synthases. Within the motif, Thr341 and Asp343 form hydrogen bonds with the polymer's terminal sugar unit, which may enable the finger helix to exert force on the polymer during the upward movement. Both residues are well-suited for this task: as a β-branched amino acid, the side chain hydroxyl of Thr is sterically restricted, and Asp343 is further rigidified by interactions with its backbone amide proton and that of the following residues, Extended Data Fig. 6.

How might the finger helix move downward without retro-translocating the glucan? N-terminal capping of α-helices with Asp residues has been shown to significantly stabilize the helical conformation in a pH dependent manner[31,32]. During catalysis, Asp343 abstracts a proton from the acceptor's C4 hydroxyl group[14], thereby likely altering its interaction with the amide protons at the N terminus of the finger helix. Thus, we speculate that the destabilization of the finger helix during glycosyl transfer enables it to refold in the 'down' position, after UDP release and subsequent deprotonation of Asp343. This notion is supported by the position of another conserved residue within the finger helix. Thr346 sits at the membrane distal side of the finger helix just three residues C-terminal of Asp343, and its side chain hydroxyl provides an alternative hydrogen bond partner for the backbone carbonyl of the preceding Glu342, Extended Data Fig. 6. Threonine residues in α-helices, in particular in hydrophobic environments, often induce helical kinks, which could facilitate the repositioning of the finger helix[33,34].

On its own, the finger helix is insufficient for cellulose translocation, which requires substrate or UDP binding and gating loop insertion into the active site. Thus, we conclude that the free energy of substrate binding energizes cellulose translocation. Additional thermodynamic driving force for translocation may be generated by the base catalyst itself. The post-translocation state is likely energetically favorable due to a strong interaction

between Asp343 and the acceptor's C4 hydroxyl. This interaction is broken upon protonation of its side chain during catalysis but re-established after polymer translocation.

Methods

In crystallo cellulose synthesis

Rhodobacter sphaeroides BcsA–B was purified and crystallized as previously described[20] by the bicelle crystallization method with the exception that gel filtration and crystallization were carried out in buffers lacking $MgCl_2$. After the crystals grew to full size (about 2 weeks), cryo-protection was initiated by 3 successive 2 uL additions of cryo solution (well solution containing 20% glycerol) to the crystal mother liquor without added $MgCl_2$, each addition separated by 10 minutes.

After the third addition of cryo solution, the polymer was elongated by adding 0.8 μL of 100 mM UDP-activated sugar (glucose or 2-fluoro glucose) in the absence of $MgCl_2$ to the ~8 μL crystallization drop for a final UDP-sugar concentration near 10 mM. The crystals were incubated with UDP-sugar for 2–3 hours at 30°C. After incubation, 6 μL of the crystallization solution was replaced with an equal volume of fresh cryo solution and this process was repeated twice to dilute the UDP-sugar concentration approximately 65-fold. Subsequently, crystals were then looped and flash-cooled in liquid N_2 at various time points.

In crystallo cellulose translocation

For *in crystallo* translocation experiments using wild-type BcsA–B, 0.8 μL of a solution containing 100 mM UDP and 250 mM $MgCl_2$ was added to the ~8 μL crystallization drop (see above) for a final concentration of ~10 mM UDP and 25 mM $MgCl_2$. Crystals were looped and flash-cooled in liquid N_2 at various time points.

For translocation experiments using the BcsA-2C mutant, cellulose was extended as described above and after completion of cryo-protection, sodium tetrathionate was added to a final concentration of ~1 mM or dithiobutylamine was added to a final concentration of ~100 mM, followed by incubation for 30 or 15 min, respectively. Then, UDP/$MgCl_2$ were added as described above, and crystals were harvested at various time points.

BcsA accepts UDP-Glc as well as UDP-Gal as substrates, however because galactose is the C4 epimer of glucose, elongation of the cellulose polymer with galactose is expected to stall after a single turn over. Thus, for translocation experiments using UDP-6-thio-Gal as substrate, polymer extension was performed as described above for other substrates with the exception that the cryo solution contained 25 mM $MgCl_2$, and the 100 mM UDP-6-thio-Gal solution contained 84 mM dithiothreitol (DTT).

Data collection

Diffraction data for wild type BcsA-B and its double cysteine mutant were collected and processed as previously described[20]. Diffraction data for UDP-6-thio-Gal were collected at 6.5 keV at NE-CAT to high redundancy. Phases were obtained by molecular replacement using a search model composed of pdb 4P02 with all ligands as well as residues 332–350 (finger helix) and 499–510 (gating loop) of BcsA omitted. All ligands except for the final 4

glucose units of the cellulose polymer were subsequently added, and the models were refined in Phenix_refine[36]. Ramachandran analyses of the product-bound, substrate-bound and pre-translocation state structures identify 95.8/3.9/0.3%, 97.6/2.4/0.0% and 96.8/3.2/0.0% residues in the preferred/allowed/outlier regions, respectively. Figures were prepared using PyMol[37] and crystallographic software is supported by SBGrid[38].

UDP-CH_2-Glc soak to generate the donor-bound state

BcsA-B was crystallized in the presence of 1 mM UDP-Gal, which was added to the protein/bicelle solution prior to mixing with the crystallization well solution. Fully-grown crystals were cryo-protected at 24°C as described above. The crystals were then incubated with cryo-solution containing 1 mM UDP-CH_2-Glc and 10 mM $MgCl_2$ for 20 minutes, harvested, and flash-cooled in liquid N_2.

Finger helix cross-linking and activity assays

BcsA cysteine mutants were generated from the constructs described earlier[10] by using the QuikChange mutagenesis technique, and the mutant BcsA-B complex was expressed and prepared as inverted membrane vesicles (IMVs) or purified and reconstituted into proteoliposomes (PLs) as previously described[7].

PLs were diluted to 125 nM (or IMVs to 12% v/v) with 125 mM NaCl and 25 mM sodium phosphate, pH 7.2, and incubated with increasing concentrations of DTT or sodium tetrathionate each for 15 minutes at 37°C, prior to initiating cellulose biosynthesis.

To initiate cellulose biosynthesis, c-di-GMP, UDP-Glc, UDP-[^{3}H]-Glc, and $MgCl_2$ were added, giving final concentrations of 100 nM BcsA-B, 20 mM sodium phosphate, pH 7.2, 100 mM NaCl, 20 mM $MgCl_2$, 5 mM UDP-Glc, 0.25 μCi UDP-[^{3}H]-Glc, and 20 μM c-di-GMP. Reactions were carried out in 25 μL aliquots at 24°C for 15 minutes, terminated by adding 2% SDS, and the tritium-labeled cellulose product was quantified by scintillation counting as previously described[7]. Reactions with IMVs containing BcsA Cys or I340 mutants were incubated at 24°C for 3 hrs or 30 min, respectively. All experiments were performed at least in triplicate as technical replicates and error bars represent the deviations from the means.

UDP-sugar syntheses

See *Supplementary Information* for detailed protocols of chemical syntheses and product characterizations.

Extended Data

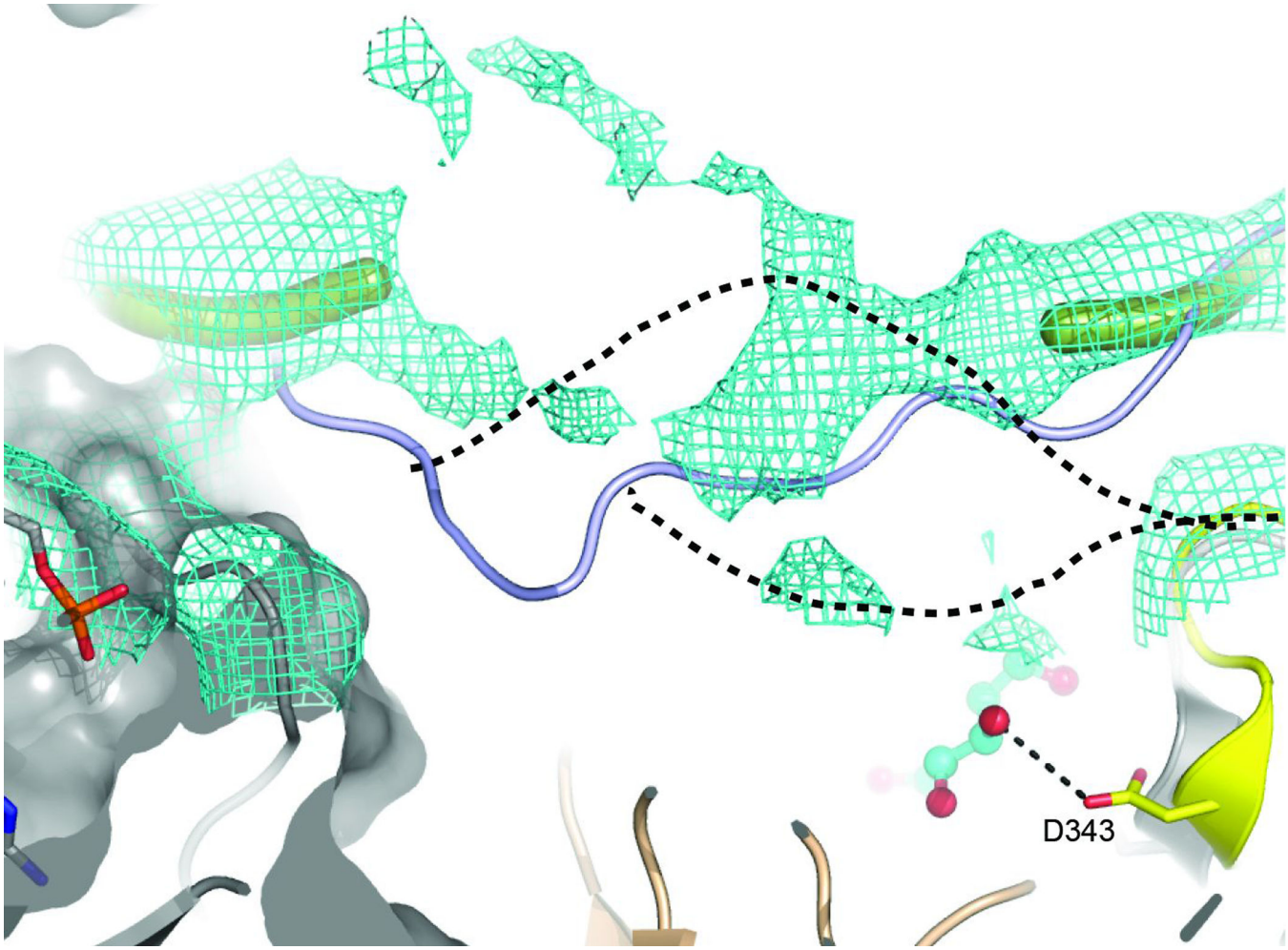

Extended Data Figure 1. Conformational flexibility of the gating loop after cellulose extension

Unbiased Sigma-A weighted Fo-Fc difference electron density of the gating loop in the pre-translocation state contoured at 2σ. The ordered part of the gating loop is shown as a thick green ribbon and two alternative backbone positions are indicated by a black dashed line. The position of the gating loop in the inserted state in the presence of a UDP molecule as observed in pdb entry 4P00 is shown as a cartoon representation colored blue.

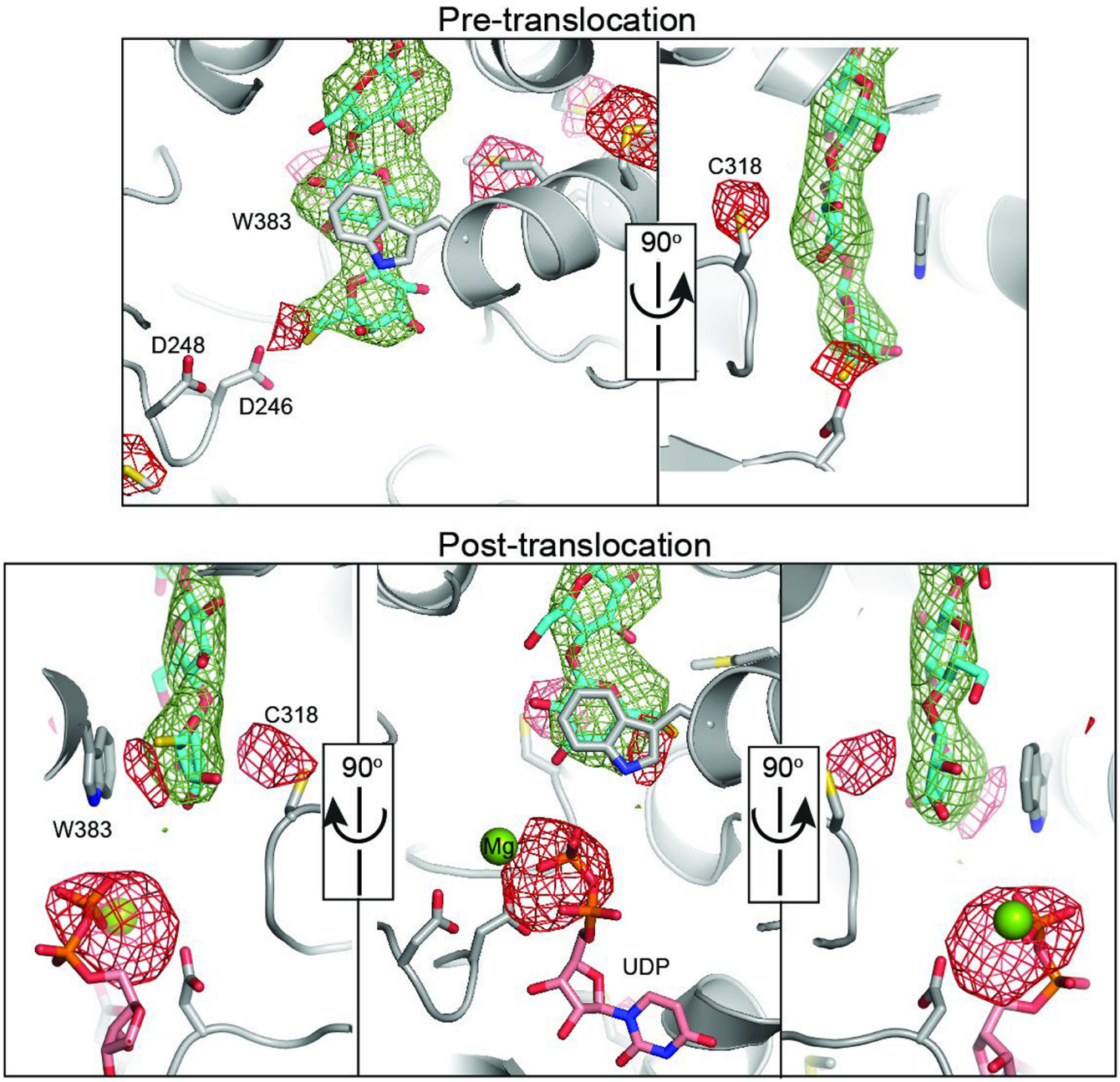

Extended Data Figure 2. ***In crystallo*** **translocation of a 6-thio-galactose-containing cellulose polymer**

The position of the 6-thio-galactose group at the polymer's non-reducing end was determined after polymer extension (upper panel) and upon subsequent incubation with UDP/Mg^{2+} (lower panel) in an anomalous difference Fourier electron density (DANO) map. DANO peaks detected at a wavelength of 1.74 Å are shown as a red mesh contoured at 3.5σ. Unbiased Sigma-A weighted Fo-Fc difference electron density for the cellulose polymer is shown as a green mesh contoured at 4σ. The cellulose polymer was extended and translocated as described in Fig. 1 with the exception that UDP-6-thio-galactose was used as substrate and Mg^{2+} was included during the initial soaking step. The extended DANO peak

around Cys318 in the post-translocation state might arise from overlapping peaks originating from Cys318 and the thio-Gal unit in an opposite orientation. All Cys and Met residues close to BcsA's active site are shown as sticks. UDP is shown as sticks in violet for its carbon atoms.

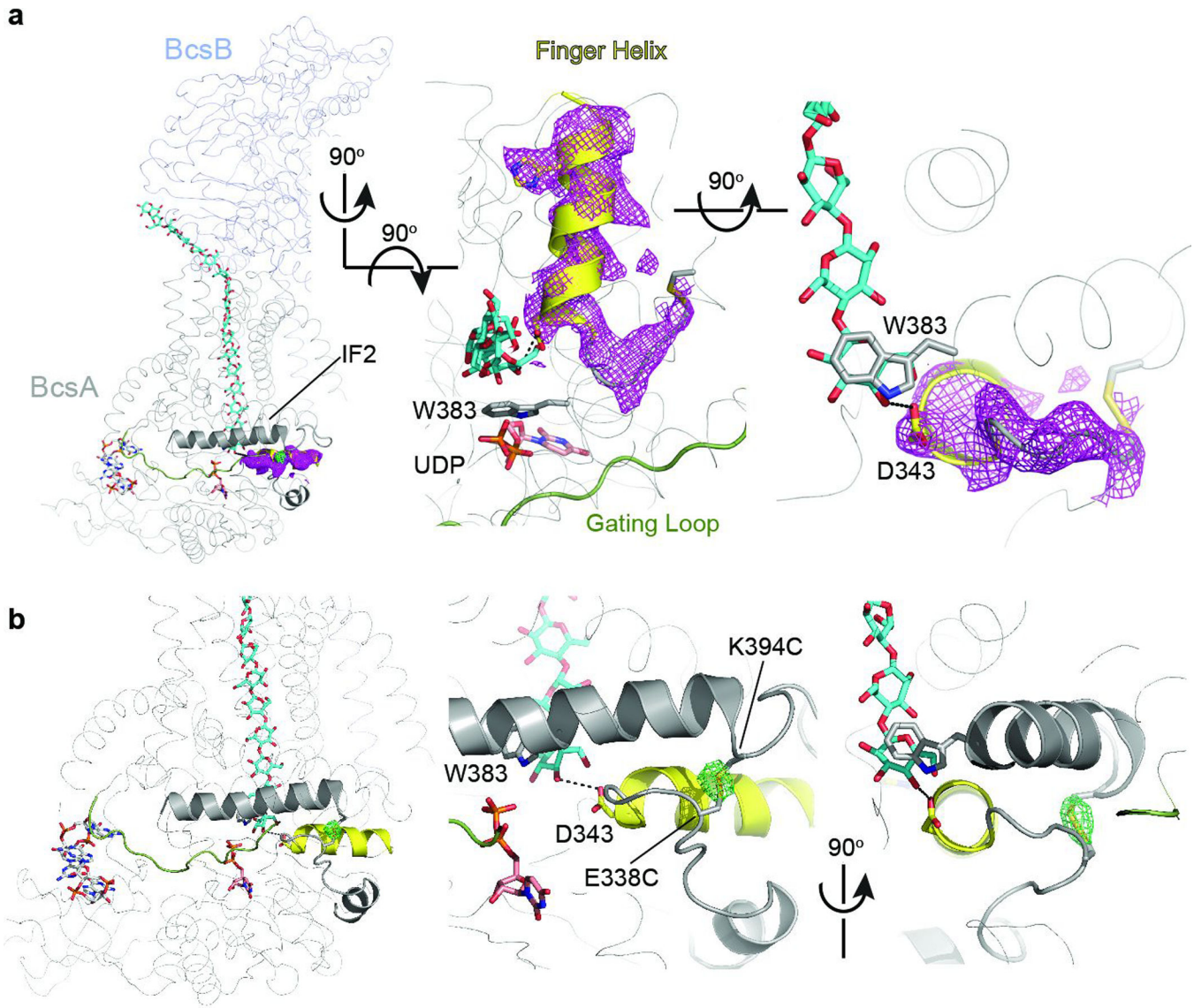

Extended Data Figure 3. Position of the disulfide-tethered finger helix

The BcsA-2C-B complex was crystallized as described for wild type BcsA-B. (**a**) Unbiased Sigma-A weighted Fo-Fc difference electron density of BcsA's finger helix contoured at 4σ (magenta mesh). Cellulose and BcsA's Trp383 at the entrance to the TM channel are shown as sticks in cyan and gray for their carbon atoms, respectively. The finger helix and IF2 are shown as cartoon helices colored yellow and gray, respectively. (**b**) The finger helix-tethered BcsA-B complex was refined in a resolution range from 34 to 3.2Å to a final R/R_{free} of 19.9/23.9% in Phenix_refine[36] with Ala residues at positions 338 and 394 of BcsA. A strong

difference electron density peak indicates the position of the omitted disulfide bond in a Sigma-A weighted Fo-Fc difference electron density map, (green mesh, contoured at 2σ).

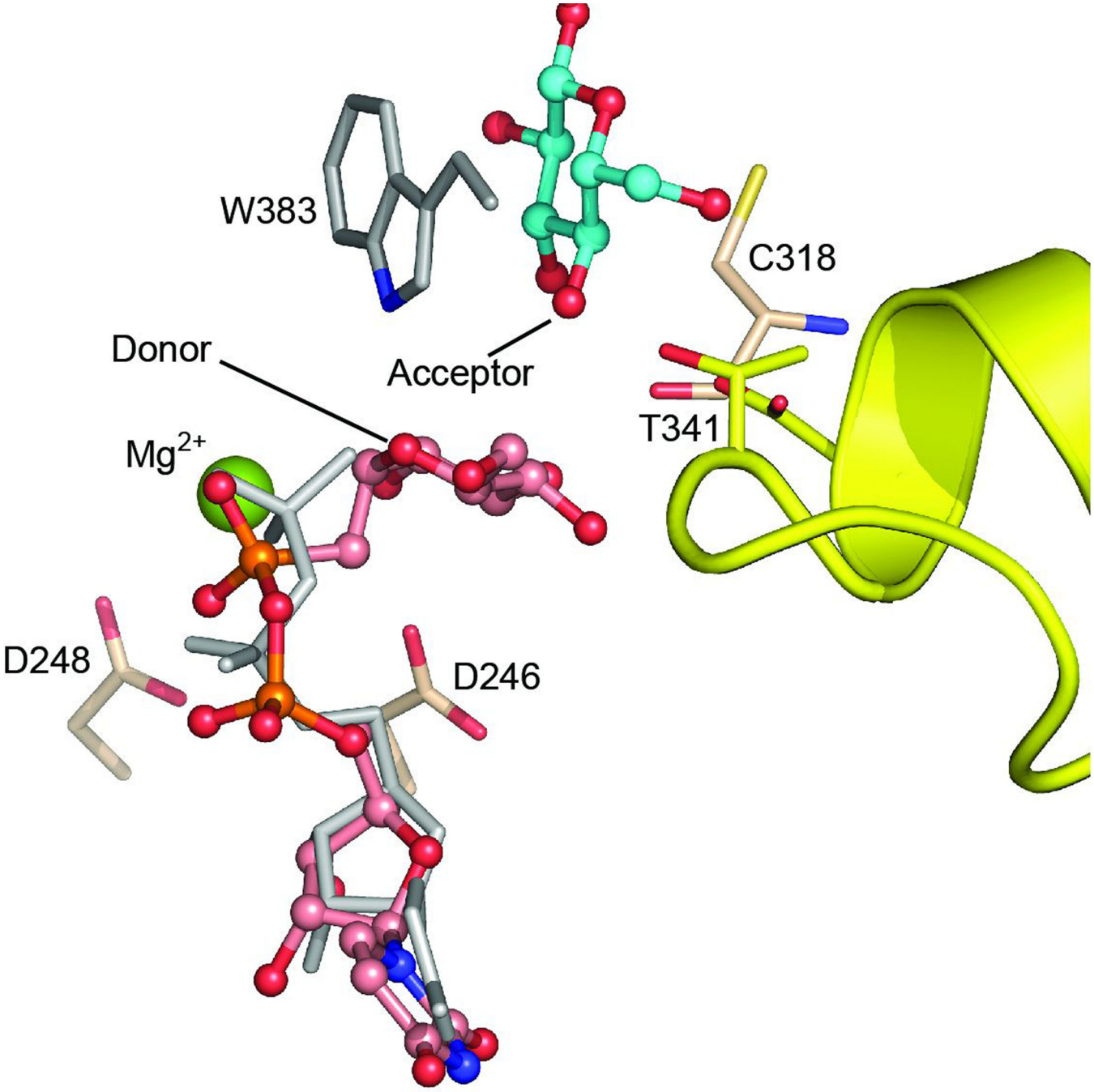

Extended Data Figure 4. Comparison of the UDP conformation in the substrate and UDP-bound states of BcsA

The substrate-bound BcsA structure was superimposed with pdb entry 4P00 by secondary structure matching in Coot. The substrate is shown as "balls and sticks" in violet for the carbon atoms and the UDP molecule from pdb entry 4P00 is shown as gray sticks. BcsA's

finger helix is shown as a yellow cartoon and the cellulose polymer is shown as cyan and red "balls and sticks" as observed in pdb entry 4P00. Magnesium is shown as a green sphere.

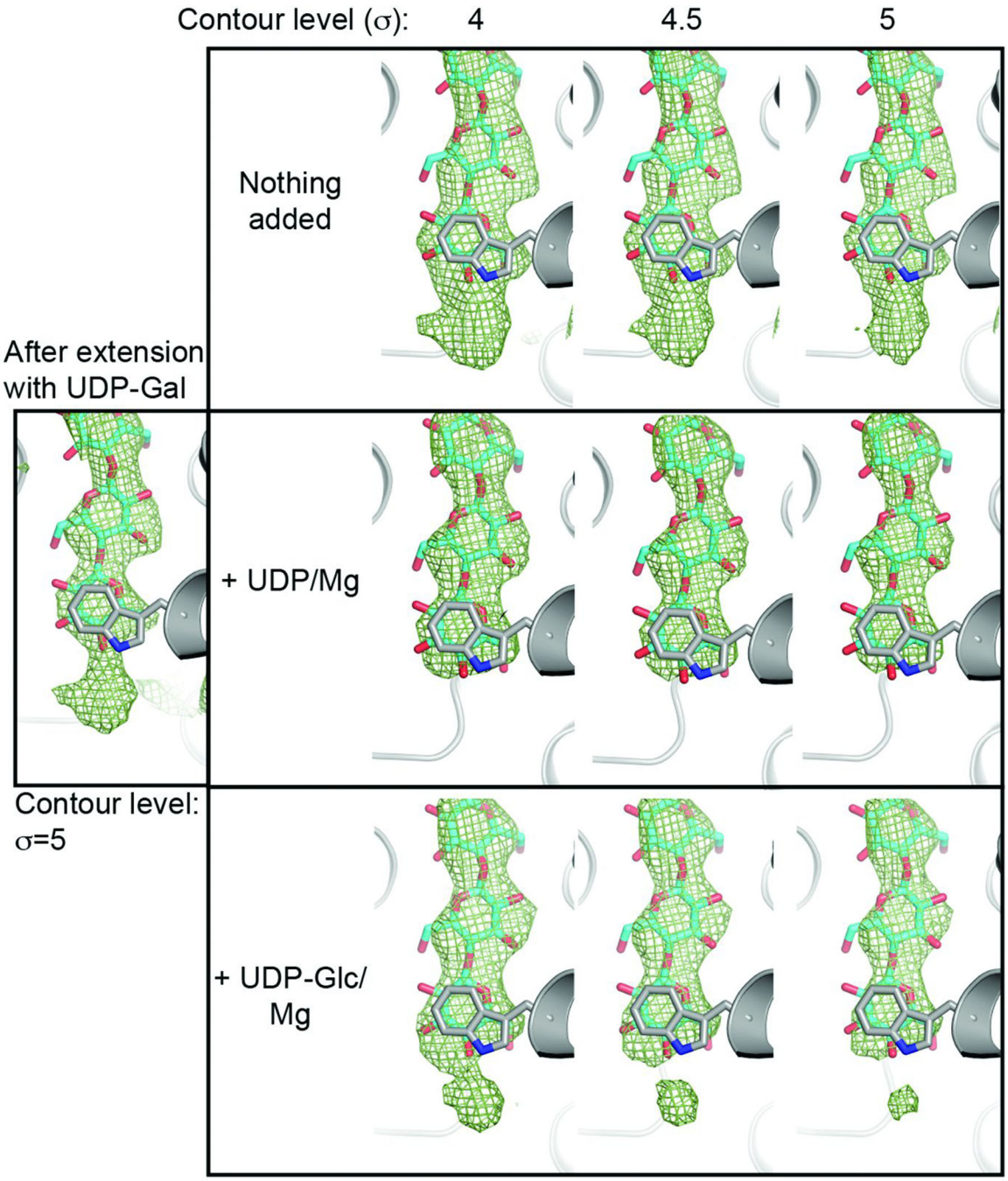

Extended Data Figure 5. UDP-Glc induced polymer translocation

The nascent cellulose polymer was extended with a chain-terminating galactose residue upon soaking BcsA-B crystals with UDP-Gal. Following dilution of the substrate as described in Fig. 1, crystals were incubated for 150 min either in the absence of a nucleotide or in the presence UDP/Mg^{2+} or UDP-Glc/Mg^{2+}, respectively. The unbiased SigmaA-

weighted Fo-Fc difference electron density of the nascent polymer (green mesh) is shown at three different contour levels, indicating that UDP-Glc also induces polymer translocation.

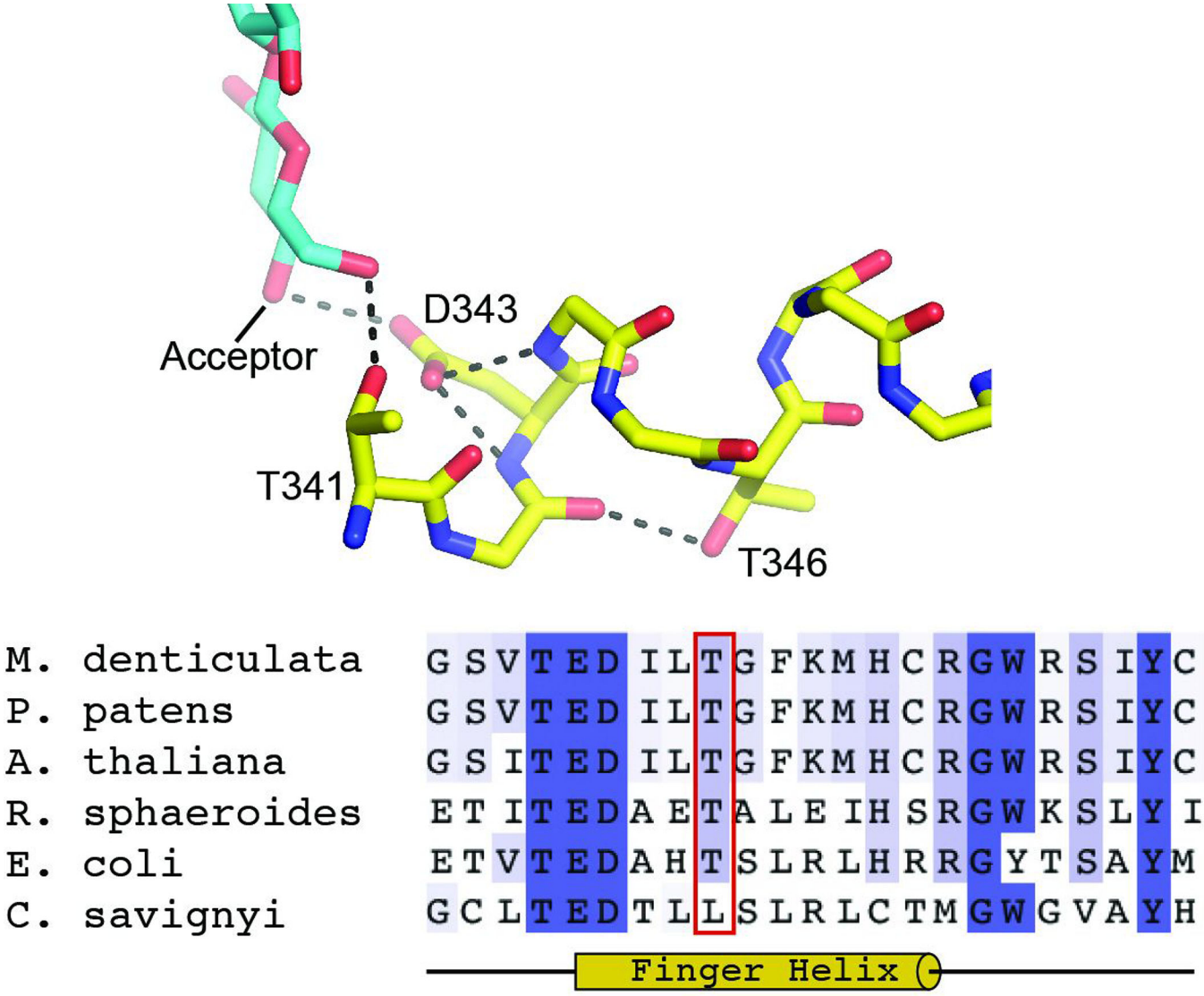

Extended Data Figure 6. Stabilization of BcsA's finger helix by conserved residues

Top panel: Stick representation of BcsA's finger helix and nascent cellulose polymer shown in yellow and cyan for their carbon atoms. The finger helix is shown as a poly-glycine helix except for the labeled residues. Bottom panel: The finger helix's "TEDxxT" motif is conserved among pro- and eukaryotic cellulose synthases. Finger helix sequences are aligned for *Micrasterias denticulata* CesA, *Physcomitrella patens* CesA5, *Arabidopsis thaliana* CesA8, *Rhodobacter sphaeroides* and *Escherichia coli* BcsA, and *Ciona savignyi* CesA. The conserved threonine following the TED motif is indicated with a red box. Of note, the threonine residue is absent from the *Ciona* CesA sequence, however, this protein contains a serine residue at the following position, which could perform a similar function.

Extended Data Table 1

Crystallographic data collection and refinement statistics.

	Product-bound	Substrate-bound	Pre-translocation
Data collection			
Space group	$P2_12_12_1$	$P2_12_12_1$	$P2_12_12_1$
Cell dimensions			
a, *b*, *c* (Å)	67.3, 216.8, 221.1	68.0 216.8 220.8	67.4 218.2 220.8
α, β, γ (°)	90, 90, 90	90, 90, 90	90, 90, 90
Resolution (Å)	39.43–2.95 (3.01–2.94) *	35.05–2.90 (2.96–2.90)	29.48–3.4 (3.52–3.4)
R_{pim}	0.060 (0.512)	0.094 (0.514)	0.056 (0.638)
$CC_{1/2}$ ^	0.995 (0.636)	0.986 (0.577)	0.997 (0.787)
Mean I / sI	10.3 (1.6)	5.2 (1.2)	9.6 (1.3)
Completeness (%)	98.6 (82.4)	99.3 (90.0)	99.7 (100.0)
Redundancy	5.0 (4.2)	10.4 (9.1)	6.6 (6.9)
Refinement			
Resolution (Å)	34.35–2.94	34.92–2.95	29.48–3.4
No. reflections			
Total	68,776	70,259	86075
R_{free}	3,429	3,329	4367
R_{work}/R_{free} (%)	20.6/23.4	20.7/24.2	22.78/26.8
No. atoms			
Protein	10,673	10,725	10,618
β-1,4 g1ucan	198	188	199
c-di-GMP	92	92	92
UDP	25		
UDP-CH_2-Glc		36	
Mg^{2+}	2	2	
Lipids	89	90	69
B-factors			
Chain A	82.8	87.41	155.0
Chain B	72.2	79.4	147.0
Chain D	91.3	106.9	211.0
β-1,4 glucan	80.4	87.7	164.3
c-di-GMP	68.8	71.4	144.7
UDP	97.3		
UDP-CH_2-Glc		79.4	
Lipids	85.6	122.4	156.0
R.m.s deviations			
Bond lengths (Å)	0.003	0.003	0.004
Bond angles (°)	0.861	0.905	1.052

* Values in parentheses refer to the highest-resolution shell.

^ Correlation between intensities from random half-data sets.

Supplementary Material

Refer to Web version on PubMed Central for supplementary material.

Acknowledgments

We thank Tom Rapoport for critical comments on the manuscript and Justin Acheson for advice on reducing BcsA-B complexes *in crystallo*. Diffraction data were collected at the Argonne National Laboratory's Advanced Photon Source (APS) beam lines 23-ID-D (GM/CA-), 22-ID (SER-) and 24-ID-C (NE-CAT). GM/CA@APS has been funded in whole or in part with Federal funds from the National Cancer Institute (ACB-12002) and the National Institute of General Medical Sciences (AGM-12006). The NE-CAT beam lines are funded by the National Institute of General Medical Sciences from the National Institutes of Health (P41 GM103403). The Pilatus 6M detector on 24-ID-C beam line is funded by a NIH-ORIP HEI grant (S10 RR029205). Data for this research was also in part collected at the APS SER-CAT beam line, a U.S. Department of Energy (DOE) Office of Science User Facility operated for the DOE Office of Science by ANL under Contract No. DE-AC02-06CH11357. J.L.W.M. is supported by a National Science Foundation Graduate Research Fellowship, Grant No. DGE-1315231. M.F. thanks the Austrian Science Fund (FWF) (J3293-B21) for an Erwin Schrödinger postdoctoral fellowship. This research was primarily supported by the National Institutes of Health, Grant 1R01GM101001, awarded to J.Z. S.G.W. thanks the Natural Sciences and Engineering Research Council of Canada for financial support.

References

1. Keegstra K. Plant cell walls. Plant Physiol. 2010; 154:483–486. [PubMed: 20921169]
2. Serra DO, Richter AM, Hengge R. Cellulose as an architectural element in spatially structured Escherichia coli biofilms. J Bacteriol. 2013; 195:5540–5554. [PubMed: 24097954]
3. Römling U. Molecular biology of cellulose production in bacteria. Res Microbiol. 2002; 153:205–212. [PubMed: 12066891]
4. Kimura S, Ohshima C, Hirose E, Nishikawa J, Itoh T. Cellulose in the house of the appendicularian Oikopleura rufescens. Protoplasma. 2001; 216:71–74. [PubMed: 11732199]
5. Nishiyama Y, Sugiyama J, Chanzy H, Langan P. Crystal structure and hydrogen bonding system in cellulose I(alpha) from synchrotron X-ray and neutron fiber diffraction. J Am Chem Soc. 2003; 125:14300–14306. [PubMed: 14624578]
6. McNamara J, Morgan JLW, Zimmer J. A molecular description of cellulose biosynthesis. Annu. Rev. Biochem. 2015; 84:17.11–17.27.
7. Omadjela O, et al. BcsA and BcsB form the catalytically active core of bacterial cellulose synthase sufficient for in vitro cellulose synthesis. Proc Natl Acad Sci U S A. 2013; 110:17856–17861. [PubMed: 24127606]
8. Brown C, Leijon F, Bulone V. Radiometric and spectrophotometric in vitro assays of glycosyltransferases involved in plant cell wall carbohydrate biosynthesis. Nat Protoc. 2012; 7:1634–1650. [PubMed: 22899332]
9. Somerville C. Cellulose synthesis in higher plants. Annu Rev Cell Dev Biol. 2006; 22:53–78. [PubMed: 16824006]
10. Morgan J, Strumillo J, Zimmer J. Crystallographic snapshot of cellulose synthesis and membrane translocation. Nature. 2013; 493:181–186. [PubMed: 23222542]
11. Bokranz W, Wang X, Tschäpe H, Römling U. Expression of cellulose and curli fimbriae by Escherichia coli isolated from the gastrointestinal tract. J Med Microbiol. 2005; 54:1171–1182. [PubMed: 16278431]
12. Whitney JC, et al. Structural basis for alginate secretion across the bacterial outer membrane. Proc Natl Acad Sci U S A. 2011; 108:13083–13088. [PubMed: 21778407]
13. Keiski C-L, et al. AlgK is a TPR-containing protein and the periplasmic component of a novel exopolysaccharide secretin. Structure. 2010; 18:265–273. [PubMed: 20159471]
14. Lairson LL, Henrissat B, Davies GJ, Withers SG. Glycosyltransferases: structures, functions, and mechanisms. Annu Rev Biochem. 2008; 77:521–555. [PubMed: 18518825]

15. Hubbard C, McNamara J, Azumaya C, Patel M, Zimmer J. The hyaluronan synthase catalyzes the synthesis and membrane translocation of hyaluronan. J Mol Biol. 2012; 418:21–31. [PubMed: 22343360]
16. Merzendorfer H. Insect chitin synthases: a review. J Comp Physiol B. 2006; 176:1–15. [PubMed: 16075270]
17. Rehm BH. Alginate Production: Precursor Biosynthesis, Polymerization and Secretion. Microbiology Monographs. 2009; 13:55–71.
18. Ross P, et al. Regulation of cellulose synthesis in Acetobacter xylinum by cyclic diguanylic acid. Nature. 1987; 325:279–281. [PubMed: 18990795]
19. Römling U, Galperin M, Gomelsky M. Cyclic di-GMP: the First 25 Years of a Universal Bacterial Second Messenger. Microbiol Mol Biol Rev. 2013; 77:1–52. [PubMed: 23471616]
20. Morgan JLW, McNamara JT, Zimmer J. Mechanism of activation of bacterial cellulose synthase by cyclic di-GMP. Nature Struct Mol Biol. 2014; 21:489–496. [PubMed: 24704788]
21. Saxena IM, Brown RM, Dandekar T. Structure--function characterization of cellulose synthase: relationship to other glycosyltransferases. Phytochemistry. 2001; 57:1135–1148. [PubMed: 11430986]
22. Persson K, et al. Crystal structure of the retaining galactosyltransferase LgtC from Neisseria meningitidis in complex with donor and acceptor sugar analogs. Nature Struct Mol Biol. 2001; 8:166–175.
23. Chan PH, et al. Investigating the structural dynamics of alpha-1,4-galactosyltransferase C from Neisseria meningitidis by nuclear magnetic resonance spectroscopy. Biochemistry. 2013; 52
24. Gardner KH, Blackwell J. The hydrogen bonding in native cellulose. Biochim Biophys Acta. 1974; 343:232–237. [PubMed: 4828858]
25. Yang H, Zimmer J, Yingling YG, Kubicki JD. How Cellulose Elongates-A QM/MM Study of the Molecular Mechanism of Cellulose Polymerization in Bacterial CESA. J Phys Chem B. 2015; 119:6525–6535. [PubMed: 25942604]
26. Carpita NC. Update on mechanisms of plant cell wall biosynthesis: how plants make cellulose and other (1->4)-beta-D-glycans. Plant Physiol. 2011; 155:171–184. [PubMed: 21051553]
27. Martin JL, Johnson LN, Withers SG. Comparison of the binding of glucose and glucose 1-phosphate derivatives to T-state glycogen phosphorylase b. Biochemistry. 1990; 29:10745–10757. [PubMed: 2125493]
28. Dougherty DA. Cation-pi interactions in chemistry and biology: a new view of benzene, Phe, Tyr, and Trp. Science. 1996; 271:163–168. [PubMed: 8539615]
29. Vocadlo DJ, Davies GJ, Laine R, Withers SG. Catalysis by hen egg-white lysozyme proceeds via a covalent intermediate. Nature. 2001; 412:835–838. [PubMed: 11518970]
30. Qasba PK, Ramakrishnan B, Boeggeman E. Structure and Function of β-1,4-Galactosyltransferase. Curr Drug Targets. 2008; 4:292–309. [PubMed: 18393823]
31. Forood B, Feliciano EJ, Nambiar KP. Stabilization of alpha-helical structures in short peptides via end capping. Proc Natl Acad Sci U S A. 1993; 90:838–842. [PubMed: 8430094]
32. Dirr HW, Little T, Kuhnert DC, Sayed Y. A conserved N-capping motif contributes significantly to the stabilization and dynamics of the C-terminal region of class Alpha glutathione S-transferases. J Biol Chem. 2005; 280:19480–19487. [PubMed: 15757902]
33. Scharnagl C, et al. Side-chain to main-chain hydrogen bonding controls the intrinsic backbone dynamics of the amyloid precursor protein transmembrane helix. Biophys J. 2014; 106:1318–1326. [PubMed: 24655507]
34. Cao Z, Bowie JU. Shifting hydrogen bonds may produce flexible transmembrane helices. Proc Natl Acad Sci U S A. 2012; 109:8121–8126. [PubMed: 22566663]
35. Cantarel B, Coutinho P, Rancurel C, Bernard T. The Carbohydrate-Active EnZymes database (CAZy): an expert resource for Glycogenomics. Nucleic Acids Res. 2009; 37:D233–D238. [PubMed: 18838391]
36. Adams P, et al. PHENIX: a comprehensive Python-based system for macromolecular structure solution. Acta Crystallogr D Biol Crystallogr. 2010; 66:213–221. [PubMed: 20124702]
37. DeLano Scientific. Sancarlos CA: PyMol.

38. Morin A, et al. Collaboration gets the most out of software. Elife. 2013; 2:e01456. [PubMed: 24040512]

39. Beaton SA, Huestis MP, Sadeghi-Khomami A, Thomas NR, Jakeman DL. Enzyme-catalyzed synthesis of isosteric phosphono-analogues of sugar nucleotides. Chem Commun (Camb). 2009:238–240. [PubMed: 19099081]

40. Withers SG, Maclennan DJ, Street IP. The Synthesis and Hydrolysis of a Series of Deoxyfluoro-D-Glucopyranosyl Phosphates. Carbohydrate Research. 1986; 154:127–144.

41. Stick VR, Watts AG. The cameleon of retaining glycoside hydrolases and retaining glycosyl transferases: The catalytic nucleophile. Monatsh. Chem. 2002; 133:541–554.

42. Lou, B.; Reddy, GV.; Wang, H.; Hanessian, S. Preparative Carbohydrate Chemistry. Marcel Dekker Inc.; 1997. p. 389-410.

43. Mukaiyama T, Takahashi K. A convenient method for the preparation of unsymmetrical disulfides by the use of diethyl azodicarboxylate. Tetrahedron Lett. 1968:5907–5908.

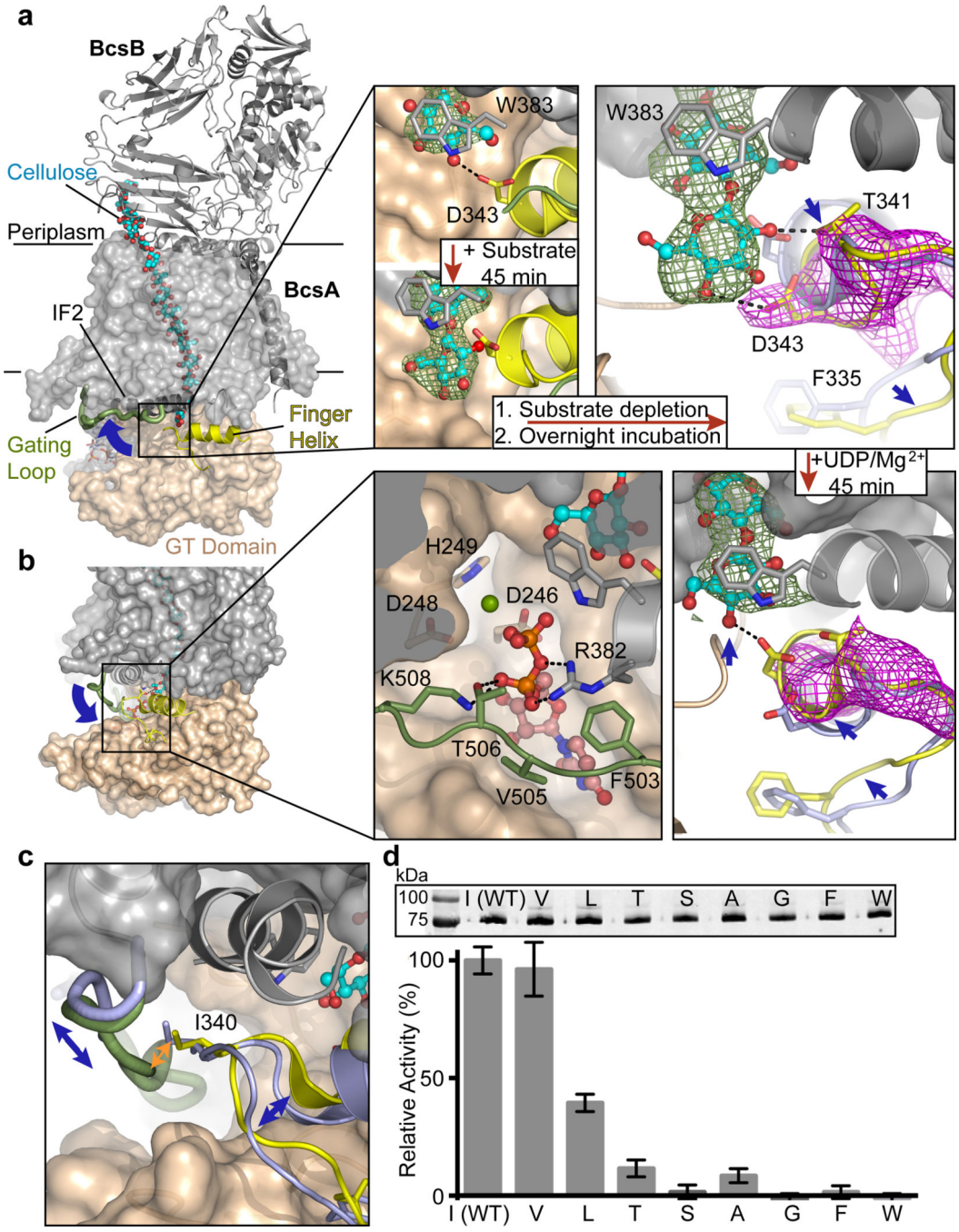

Figure 1. ***In crystallo*** **cellulose biosynthesis**

BcsA is shown as a surface with the TM and GT regions colored gray and beige. BcsB is shown as a gray cartoon. The cellulose polymer is shown as cyan sticks, BcsA's finger helix and gating loop are shown as a cartoon colored yellow and green, respectively. Trp383 is represented in gray sticks as a marker for the TM channel entrance. (**a**), Left Panel: Organization of the BcsA-B complex and formation of a channel for the translocating polymer. Right Panel: The pre-translocation state of BcsA. Unbiased Sigma-A weighted Fo-Fc difference electron densities contoured at 4 and 3σ are shown as green and magenta

meshes for the nascent cellulose chain and finger helix, respectively. (**b**) Translocation of cellulose. Crystals described in (a) were subsequently soaked with UDP/Mg^{2+}. UDP is shown in sticks and colored violet for the carbon atoms and Mg^{2+} is shown as a green sphere. (**c**) Insertion of the gating loop into the active site is incompatible with the ‘down’ position of the finger helix, likely due to a clash between Ile340 and the gating loop's backbone. The retracted gating loop and finger helix in the ‘down’ position are both shown as blue cartoons. (**d**) Cellulose biosynthesis by BcsA I340 mutants. Ile340 was replaced with the indicated residues and *in vitro* cellulose biosynthesis was performed in IMVs as described[7]. All activities are represented relative to the WT activity. All experiments were performed at least in triplicate and error bars represent standard deviations from the means. Inset: Western analysis of the IMVs used, showing equal expression levels of all BcsA mutants.

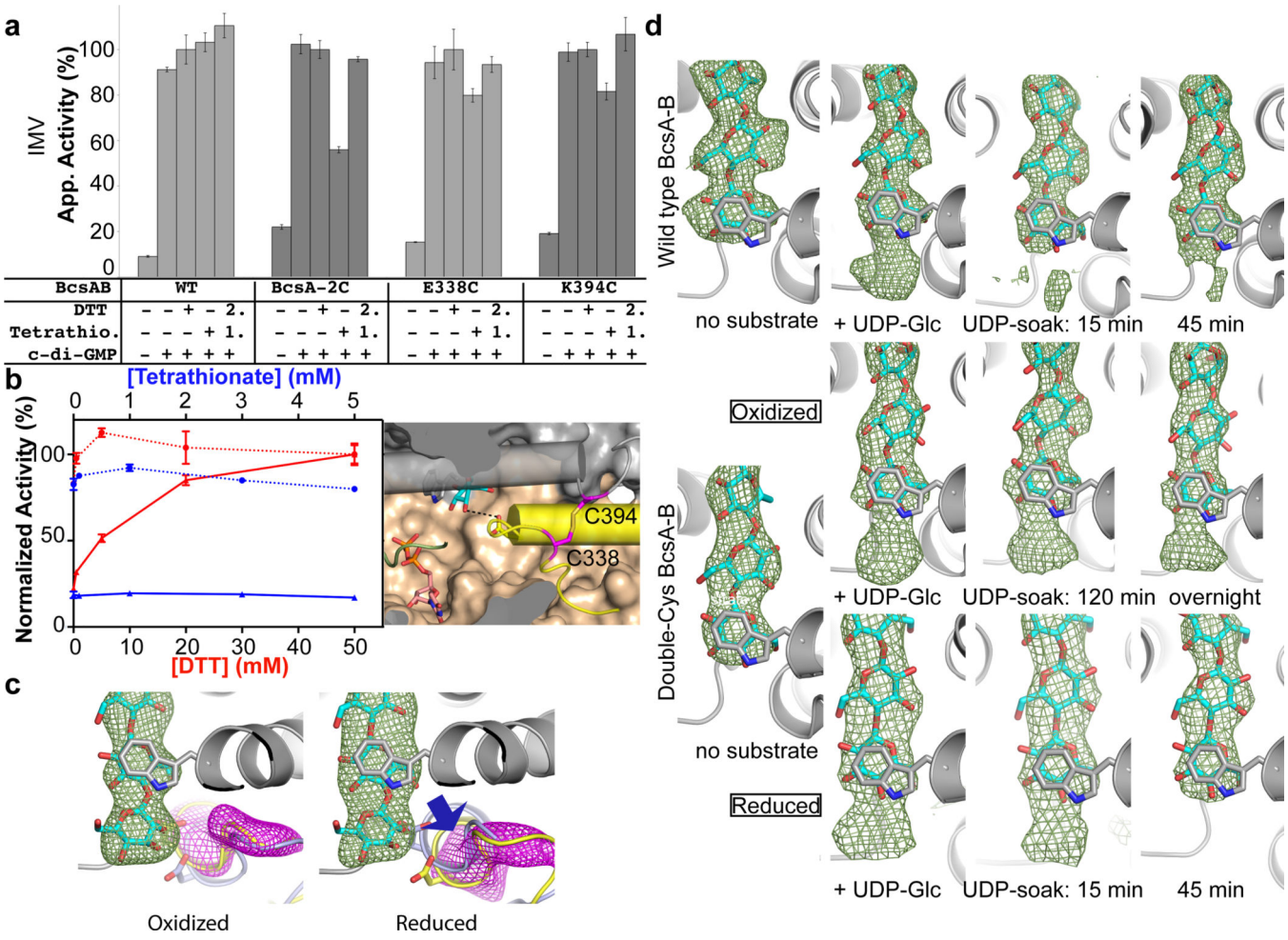

Figure 2. Movement of BcsA's finger helix is essential for cellulose translocation

In vitro cellulose formation by wild type and mutant BcsA-B complexes. (**a**) Activity in IMVs under reducing (DTT) and oxidizing (sodium tetrathionate) conditions. For each mutant tested, the apparent activity was normalized to its activity in the presence of 50 mM DTT and (1.) and (2.) indicate the order of DTT and tetrathionate addition. (**b**) DTT and tetrathionate titrations are shown in red and blue, respectively, for wild type BcsA (dashed lines) and BcsA-2C (solid lines). All experiments were performed at least in triplicate and error bars represent the deviations from the means. Right panel: Location of the engineered disulfide bond in BcsA-2C, colored as in Fig. 1. (**c**) Comparison of BcsA-2C finger helix positions following polymer extension under oxidizing and reducing conditions. Upon cellulose elongation, crystals were oxidized or reduced and incubated without substrate for 16 hrs or 6 hrs, respectively. (**d**) Comparison of *in crystallo* cellulose translocation in WT and BcsA-2C. The cellulose polymer was extended, then translocation was initiated as described in Fig. 1, and crystals were harvested after the indicated incubation periods. In all panels, the unbiased electron densities for the glucan and finger helix are contoured and colored as described in Fig. 1. Trp383 of the acceptor-binding site is shown in gray.

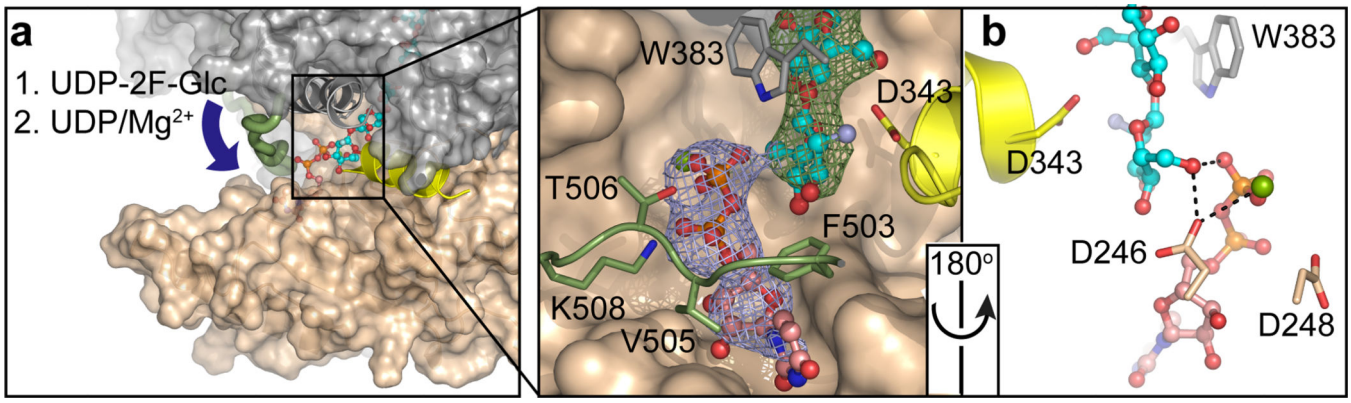

Figure 3. The product-bound state

The product-bound state of BcsA contains an elongated cellulose polymer and an inserted gating loop coordinating UDP/Mg^{2+} at the active site. (**a**) Cellulose was elongated *in crystallo* with a 2-deoxy-2-fluoro-glucose moiety and UDP/Mg^{2+} was rebound to the active site as described in Fig. 1. Unbiased Sigma-A weighted Fo-Fc difference electron densities contoured at 4 and 4.5σ are shown for the nascent cellulose polymer and UDP/Mg^{2+} in green and blue, respectively. (**b**) The terminal glucose unit of the extended cellulose polymer forms interactions with the β-phosphate of UDP and Asp246 of the DxD motif. Colors are as in Fig. 1 and fluorine is shown in light blue.

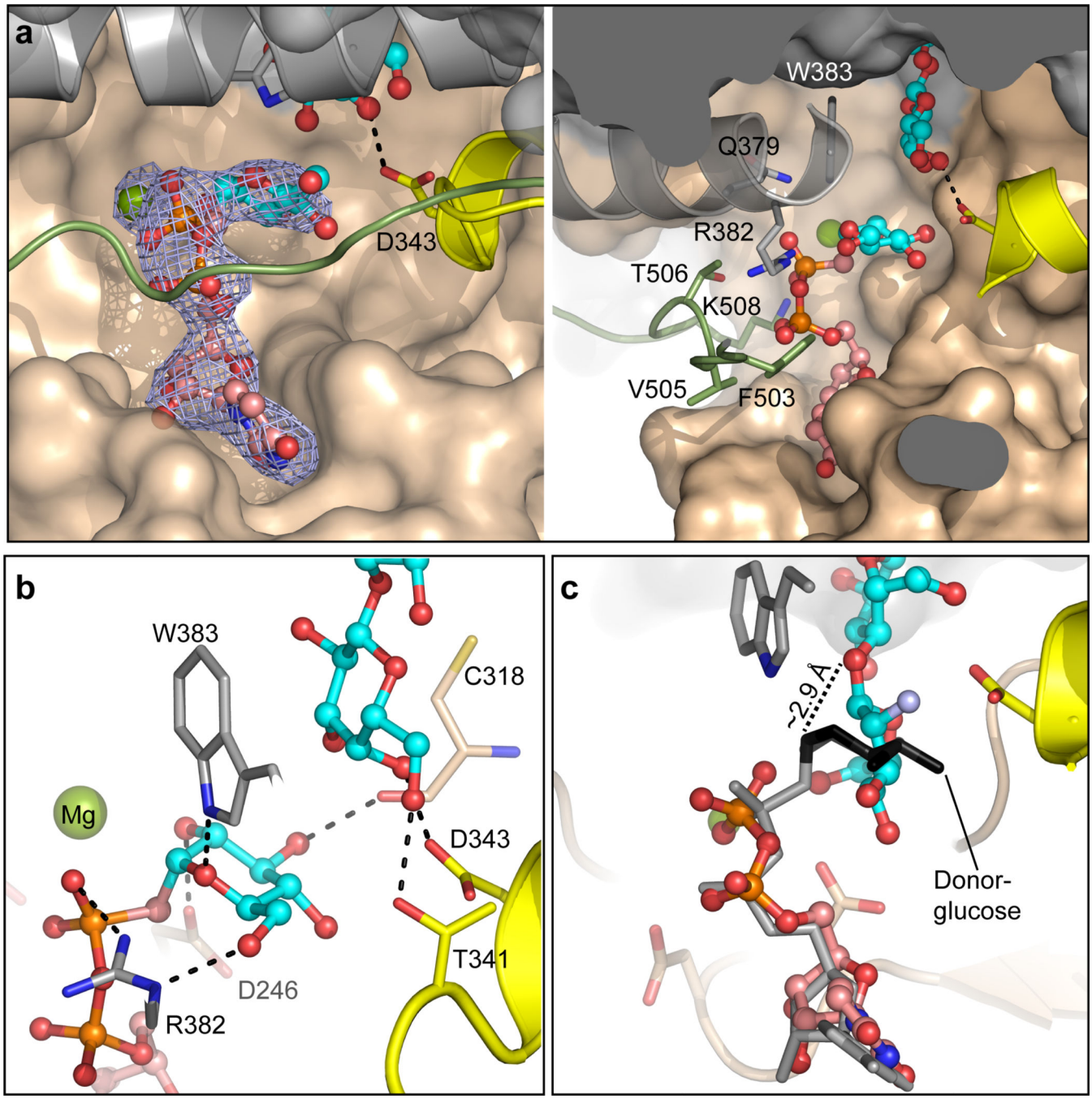

Figure 4. The substrate-bound state

The donor glucose binds in a conserved pocket beneath the acceptor. (**a**) Unbiased Sigma-A weighted Fo-Fc difference electron density of UDP-CH_2-glucose at BcsA's active site, contoured at 4σ. Right panel: Conserved residues of BcsA involved in coordinating the donor glucose are shown as sticks. (**b**) Interactions between the donor sugar moiety and BcsA's D_{246}xD, $FFC_{318}GS$, $T_{341}ED_{343}$ and $QxxR_{382}W_{383}$ motifs. (**c**) Comparison of substrate- and product-bound states. Aligning the substrate's pyrophosphate group with the position of UDP in the product-bound state (Fig. 3) positions the donor's C1 carbon within

approximately 2.9 Å of the acceptor's hydroxyl group. The substrate is shown as gray and black sticks for its UDP and glucose moieties, respectively.

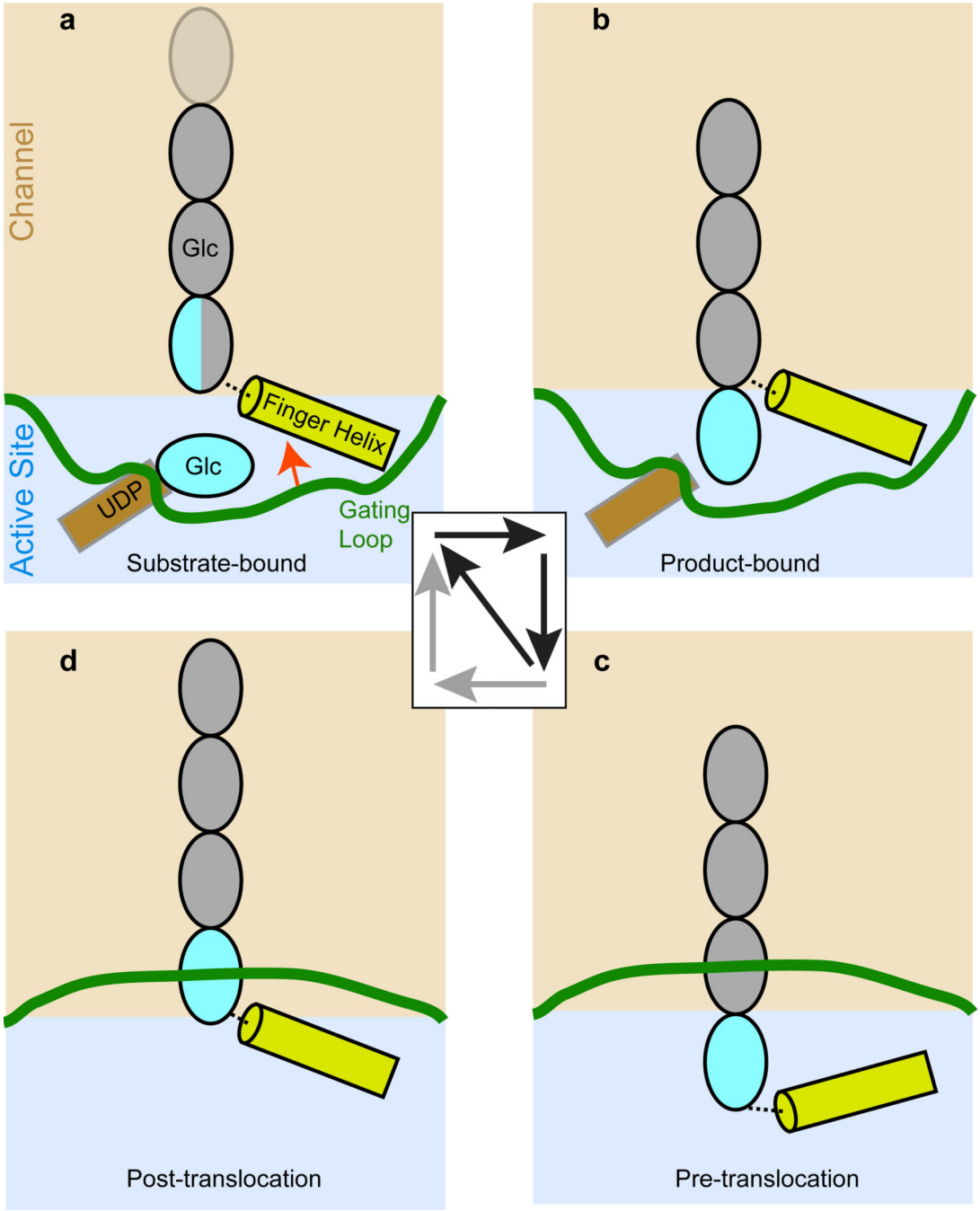

Figure 5. Model of cellulose biosynthesis

Cellulose biosynthesis might start with substrate binding to BcsA when the polymer's terminal glucose unit sits at the acceptor site at the entrance to BcsA's TM channel (a). At this time, the gating loop stabilizes the substrate and the finger helix in the ‘up’ position (red arrow). Glycosyl transfer generates the product-bound state (b) and retraction of the gating loop and UDP release allows the finger helix to reset to the ‘down’ position to contact again the polymer's terminal glucose unit (c). Substrate binding to this pre-translocation state and insertion of the gating loop could induce the upward movement of the finger helix and

polymer translocation (a) or spontaneous translocation might precede substrate binding via a post-translocation state (d).